




Functional roles of coral reef primary producers examined with stable isotopes

Sara Godinez-Espinosa^A , Vincent Raoult^B , Timothy M. Smith^{B,C} , Troy F. Gaston^B  and Jane E. Williamson^{A,*} 

For full list of author affiliations and declarations see end of paper

***Correspondence to:**

Jane E. Williamson
School of Natural Sciences, Macquarie University, Sydney, NSW 2109, Australia
Email: jane.williamson@mq.edu.au

Handling Editor:

Melanie Bishop

Received: 8 August 2022

Accepted: 11 April 2023

Published: 3 May 2023

Cite this:

Godinez-Espinosa S *et al.* (2023)
Marine and Freshwater Research, **74**(7),
601–613.
doi:[10.1071/MF22103](https://doi.org/10.1071/MF22103)

© 2023 The Author(s) (or their employer(s)). Published by CSIRO Publishing.
This is an open access article distributed under the Creative Commons Attribution-NonCommercial-NoDerivatives 4.0 International License (CC BY-NC-ND).

OPEN ACCESS

ABSTRACT

Context. Primary production on coral reefs varies under changing conditions such as light and nutrient availability. This variation causes changes in basal stable isotopes as photosynthetic and nutrient pathways change. **Aims.** This study provides a preliminary baseline of nitrogen ($\delta^{15}\text{N}$) and carbon ($\delta^{13}\text{C}$) stable isotope profiles in *Symbiodinium* and macroalgae at a spatial scale and along a depth gradient around an island. **Methods.** Coral fragments and macroalgae were collected at depths from the surface to 26 m. $\delta^{15}\text{N}$ and $\delta^{13}\text{C}$ stable isotope values were assessed for *Symbiodinium* relative to cell density per surface area. **Key results.** $\delta^{15}\text{N}$ values showed a uniform nutrient profile across primary producers. However, chlorophyll-*a* and *Symbiodinium* density from *Montipora stellata* had higher concentrations on the southern side of the island. $\delta^{15}\text{N}$ values of *Symbiodinium* from *Stylophora pistillata* and macroalgae did not change with depth. Depth was associated with a significant decrease in *Symbiodinium* density, and $\delta^{13}\text{C}$ values in macroalgae. **Conclusions.** We attribute these findings to *Symbiodinium* from *S. pistillata* as depth increases, decreasing cell density but maintaining chlorophyll-*a* concentration to satisfy the coral-host nutrient requirements. **Implications.** This study sets the scene for future, more comprehensive research on detecting carbon and nitrogen stable isotope values on primary producers in coral reefs.

Keywords: carbon, depth, macroalgae, nitrogen, nutrient, nutrients, photogrammetry, primary productivity, SIA, stable isotope baseline, *Symbiodinium*, Vanuatu.

Introduction

Primary production in tropical coral reefs occurs from a range of organisms, including corals and macro-, epiphytic and symbiotic algae. The rate of primary production is dictated by environmental factors and an organism's ability to adapt or acclimate under local conditions (Hoey *et al.* 2016; Baums *et al.* 2019). Changes in light and nutrient availability are key drivers of primary production in coral ecosystems that can alter photosynthetic and nutrient pathways of primary producers (Brandl *et al.* 2019; Johnson *et al.* 2020). However, the response of primary producers to environmental changes is unlikely to be uniform and may depend on the type of species and magnitude of change (Perry *et al.* 2011).

Scleractinian corals are sensitive to environmental change, particularly variations in local nitrogen (Lapointe 1997; Hoegh-Guldberg and Williamson 1999) and light (Tremblay *et al.* 2015) availability. Environmental change can modify coral metabolism (Fabricius 2005) and growth (Carricart-Ganivet *et al.* 2000), which are then reflected in changes to their soft tissue and preserved skeletal structure (Wheeler and Björnsäter 1992; Chan *et al.* 2016; Mollica *et al.* 2018). The relationship between host corals and their endosymbiotic zooxanthellae is complex and also depends on environmental conditions (Baker 2003). Carbon and nitrogen are essential for *Symbiodinium* photosynthesis, and for the translocation of organic molecules to the coral host (Ezzat *et al.* 2017). Photosynthetic rates for *Symbiodinium* are generally higher in shallow water and high light conditions (Reynaud *et al.* 2009), whereas photosynthetic production conversely decreases under diminishing light conditions and increasing depths (Gattuso *et al.* 1993; Anthony and Fabricius 2000).

However, *Symbiodinium* in some species of coral can uncouple this relationship and maintain or increase their photosynthetic activity in low light conditions (Lesser et al. 2010; Seemann et al. 2012). Light thus plays a key role in regulating the amount of carbon translocated from *Symbiodinium* to the coral host, facilitating respiration and growth (Ezzat et al. 2017). This is particularly important in shallow-water corals because photosynthetically-fixed carbon from *Symbiodinium* may provide $\geq 70\%$ of their daily carbon budget (Tanaka et al. 2006). This relationship between scleractinian corals and *Symbiodinium*, and their patterns of interactions with abiotic parameters, offers an opportunity to use corals as bioindicators to assess changes in water quality, trace-nutrient inputs, and nutrient recycling (Reynaud et al. 2009).

Macroalgae grow alongside coral on many reefs and can act as bioindicators of nitrogen by providing accurate records of nitrogen assimilation (Umezawa et al. 2002) and temporal information of biologically available nitrogen in the environment (Costanzo et al. 2001). Although being similar in their use as bioindicators, corals and macroalgae differ in the way they assimilate nitrogen. Macroalgae readily assimilate nutrients directly from the water column (Koop et al. 2001) or from heterotrophs (Williamson and Rees 1994), whereas uptake in hermatypic corals depends on nutrient recycling with their symbiotic algae, in addition to nutrient availability in the water column (Grottoli et al. 2006; Tanaka et al. 2010). It is therefore expected that stable isotope signatures of macrophytes will directly relate to exogenous nutrient availability, whereas the nutrient recycling that occurs in coral tissues will act as a mediator to environmental conditions. Because of this, one can also hypothesise that nutrient signatures of algae, such as macroalgae and their associated algal epiphytes, that are directly exposed to the external environment would differ when compared with those of coral endosymbiotic algae in the same habitat.

Stable isotopes are widely used to examine photosynthetic, nutrient and carbon pathways in marine environments such as coral reefs (Risk et al. 2009; McMahan et al. 2016; Eurich et al. 2019; Koweek et al. 2019). In corals, nitrogen isotopes can discriminate natural and anthropogenic sources of nitrogen, and trophic level by associating the degree of autotrophy or heterotrophy (Owens 1988; Muscatine et al. 2005; Risk et al. 2009). Similarly, carbon stable isotopes can be used as a tool to discriminate carbon fixation pathways (Fry and Sherr 1989; Seemann 2013). The effects of depth on coral and macroalgal stable isotopes have been examined (Sherwood et al. 2008; Alamaru et al. 2009); yet, the effects of depth and mixotrophy on the stable isotope values of *Symbiodinium* are not well understood.

Little is known of the status of the coral reefs in the Republic of Vanuatu ('Vanuatu'). Vanuatu is considered a Small Island Developing State (SIDS), which is typified by a vulnerability to impacts associated with climate change, such as an increase in the frequency of extreme weather events, coastal erosion, increases in water temperature, and coral

bleaching (Buckwell et al. 2020). For example, bleaching events in Vanuatu caused mass mortality of corals in 2002, and Cyclone Pam caused severe damage to 80% of hard corals in 2015 (Sulu 2007; Burke et al. 2012). In addition, Vanuatu does not harbour a sophisticated sewage treatment system, and much of the terrestrial waste occurs as runoff into adjacent reefs (Mosley and Aalbersberg 2003). These make Vanuatu, and particularly the island of Efate where the majority of Nivans reside, an interesting location for analysing the nutrient profiles of key reef-associated primary producers by using stable isotope analysis.

Here we examined spatial changes in nutrient sources of *Symbiodinium* from two common scleractinian corals and associated algae on a shallow coral lagoonal reef in Vanuatu by using stable isotope analysis (SIA). The following questions were asked: (1) can SIA detect spatial changes in nutrient signatures (i.e. nitrogen and carbon) for primary producers on a lagoonal reef at a medium scale (i.e. zones around a small island, north, south, east, west); (2) do nutrient profiles of coral endosymbionts differ from those of adjacent macroalgae and epiphytes in a shallow coral lagoonal reef; and (3) does depth influence any nutrient uptake detected in *Symbiodinium*, macroalgae or epiphytes? For the second question, we hypothesised that in the shallow reef waters, endosymbiotic algae within corals would maintain a uniform nutrient profile because of nutrient recycling between *Symbiodinium* and the coral host, whereas the nutrient profile of macroalgae (and their epiphytes) would exhibit greater variation linked to exogenous nutrient availability. Finally, we hypothesised that nutrient availability would change as depth increased and light decreased, driving differences in N and C isotopic signatures for macroalgae and epiphytic algae, but not for *Symbiodinium* because their ability to compensate by increasing chlorophyll-*a* (Chl-*a*) concentration and cell density in the coral host.

Materials and methods

Study site and sample collection

Endosymbiotic algae, macroalgae and epiphytes were sampled from the shallow fringing reef surrounding Hideaway Island (17°41'49.2324"S, 168°15'49.0788"E) located in Mele Bay, Efate, Vanuatu, in December 2017 (Fig. 1). Mele Bay is among the more adversely affected sites in Vanuatu (Mosley and Aalbersberg 2003), receiving pollution and high nutrient-load discharges from Tagabe River, including septic runoff (Poustie and Deletic 2014). Additionally, Hideaway Island is located at the mouth of two freshwater rivers that discharge to the north-west and north-east of Hideaway Island. Ten sites were chosen across the reef flat at Hideaway Island, and subsequently categorised into zones according to their cardinal locations in relation to Hideaway Island (western, eastern and

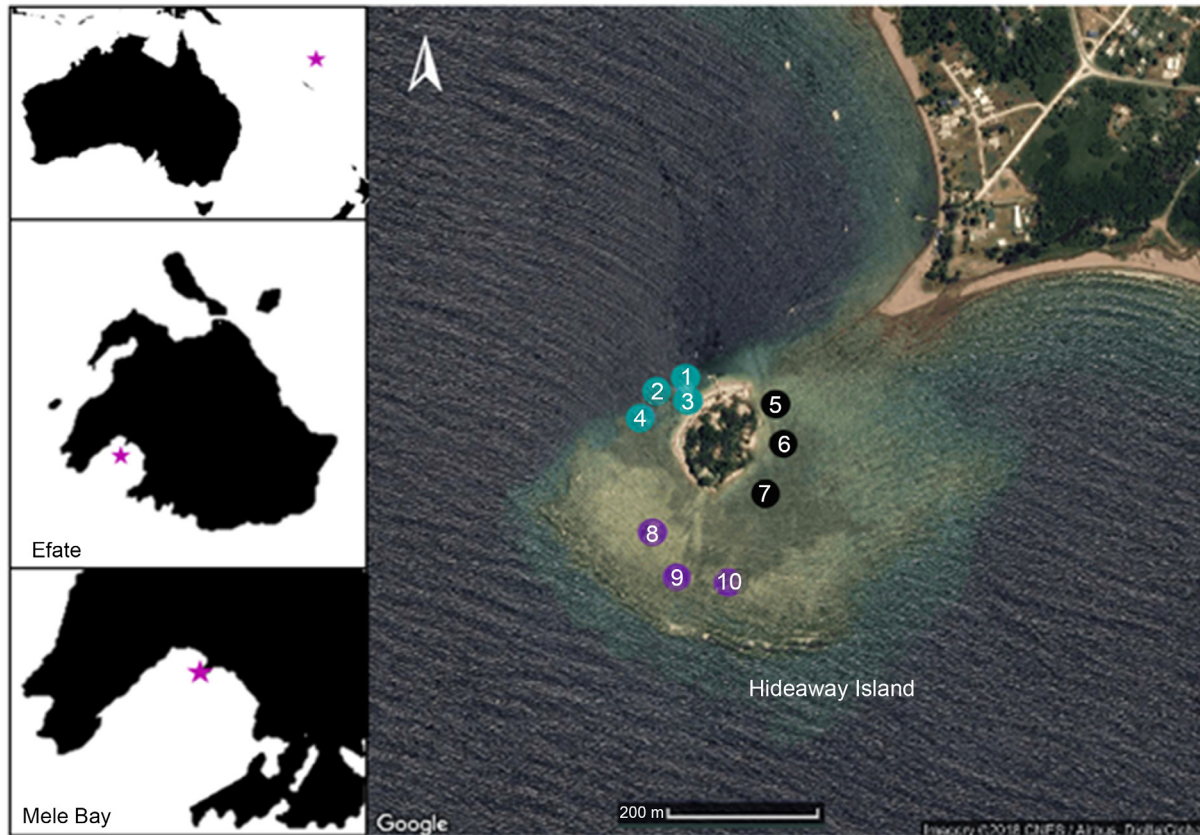


Fig. 1. Hideaway Island ($17^{\circ}41'49.2324''S$, $168^{\circ}15'49.0788''E$), Vanuatu. Eastern collection zones are shown in black, southern zones in purple, and western zones in blue. Collection sites are numbered from 1 to 10. Depth sampling occurred on the south-western end of the reef wall, between the southern and western zones. Image courtesy of Google Earth.

southern). North of the island was excluded from sampling because of a lack of fringing reef in that direction.

The branching scleractinian coral *Montipora stellata* and a mix of two species of macroalgae, namely, *Actinotrichia fragilis* and *Galaxaura rugosa*, commonly occur on the reef flat surrounding Hideaway Island (T. M. Smith, 2017, pers. obs.). These macroalgae routinely occur together and typically contain small amounts of attached epiphytic algae. This coral (known to harbour endosymbiotic algae), and macroalgae were haphazardly collected at the 10 sites along the reef flat. At each site, three small fragments of live *M. stellata* (~5-cm tip of a branch) were removed on snorkel at 1-m depth from healthy colonies (Fig. 1) for stable isotope analysis. To ensure that the primary producers came from the same microenvironment, the macroalga closest to the sampled coral was also identified and removed. After collection, all coral and macroalgal samples were placed in individual resealable bags and immediately frozen at -20°C until processing.

To assess the effect of depth on primary producers, one coral fragment (~5 cm tip of a branch) and one adjacent macroalga were collected haphazardly at each depth, while swimming in a zig-zag pattern from depth to the surface over a depth gradient ranging from 26 to 3 m on SCUBA at

the south-western area of Hideaway Island. This area was chosen because of its depth profile, but also because it was one of the more distant areas from the river mouths. Because few or no *M. stellata* colonies could be found at depths greater than 3 m on the reef slope, the scleractinian coral *Stylophora pistillata*, which occurred across this depth gradient, was sampled instead. Similarly, *G. rugosa* was not found across the depth gradient; however, *Amphiroa rigida* and *A. fragilis* were consistently present; therefore, the closest macroalgal mix of these species to the sampled coral at each depth was collected. Samples were immediately individually bagged and frozen at -20°C until processing.

Symbiodinium preparation

In the laboratory, coral host and endosymbiont tissue were removed from the calcium carbonate skeleton for each coral fragment by using a Waterpik Ultra Water Flosser filled with reverse-osmosis (RO) water. The resulting slurry for each sample was placed in a 50-mL centrifuge tube and homogenised using a knife mill (Retsch GM200) set to Speed 2 for 5 min. Three aliquots of 1 mL were separated from the resulting homogenised slurry of each sample to assess *Symbiodinium*

density. Additionally, three aliquots of 1.5 mL were taken from each slurry to perform measurements of Chl-*a* concentration. The remaining slurry samples containing host tissue and *Symbiodinium* were centrifuged (Eppendorf 5810 R) at 1700g and ambient temperature for 5 min to separate the host tissue from *Symbiodinium*. To ensure all coral host tissue was removed, the pellet containing *Symbiodinium* was resuspended with 5 mL RO water followed by centrifugation at 600g for 5 min (Wong et al. 2017). *Symbiodinium* pellets were oven dried at 60°C for 48 h, then ground to a fine powder by using a mortar and pestle, and a quantity of 1–2 mg of each sample was weighed into tin capsules for isotope analysis.

To determine the density of symbiont cells in the coral fragments, eight replicate counts were conducted from each 1-mL aliquot collected above from each sample. Aliquots (10 µL) from the coral host tissue–*Symbiodinium* slurry were added to a 0.1-mm-deep Improved Neubauer Haemocytometer and cells were counted immediately under a light microscope at 40× magnification (Olympus BX51, Japan). The 1.5-mL aliquots of the homogenised coral host tissue–*Symbiodinium* slurry of each sample were centrifuged (Eppendorf 5810 R) at 600g for 5 min in a 3-mL tube. The supernatant was discarded and the pellets containing *Symbiodinium* cells were used to extract Chl-*a*. A volume of 1 mL of cold 100% acetone was added to each *Symbiodinium* sample. Pigments were then extracted for 24 h at 4°C (Grottoli et al. 2004). The absorbance of *Symbiodinium* extract was measured at 630, 660 and 750 nm by using a spectrophotometer (SPECTROstar Nano, BMG Labtech Plate Reader), and the Jeffrey and Humphrey (1975) equation for dinoflagellates was used to standardise the Chl-*a* concentration.

Surface-area determination for coral

Determination of surface area for coral fragments was important to estimate endosymbiotic algal densities and Chl-*a* concentration. Structure from motion photogrammetry (House et al. 2018) was used to determine the surface area of each coral fragment. Each individual coral fragment was placed on a rotating table next to a 3 × 3-cm scale and overlapping photographs were taken while rotating the sample in a clockwise direction. Image processing was performed using Agisoft Photoscan Professional (ver. 1.2.5, Agisoft LLC, Saint Petersburg, Russian Federation). Images were aligned using the high to medium accuracy setting, with a key point limit of 40 000 and a tie point limit of 1000. Previous research on similar coral morphology showed no difference in accuracy between the high and medium settings (Raoult et al. 2017). The software then determined the camera position and generated points into a three-dimensional space (Fig. 2). This was followed by the generation of a dense point cloud, again by using the medium to high quality and an aggressive depth filtering. Once the point cloud was generated, a mesh was built from the overlapping images with the following settings: arbitrary surface type, dense cloud source data, high face count, and enabled (default) interpolation. On completion of the mesh build, two markers were placed on the limits of the 3 × 3 square scale to create a scale bar. The model of the coral fragment was then manually trimmed from the rest of the mesh under high resolution, and any holes in the mesh were closed by using the mesh tool, as per Raoult et al. (2017).

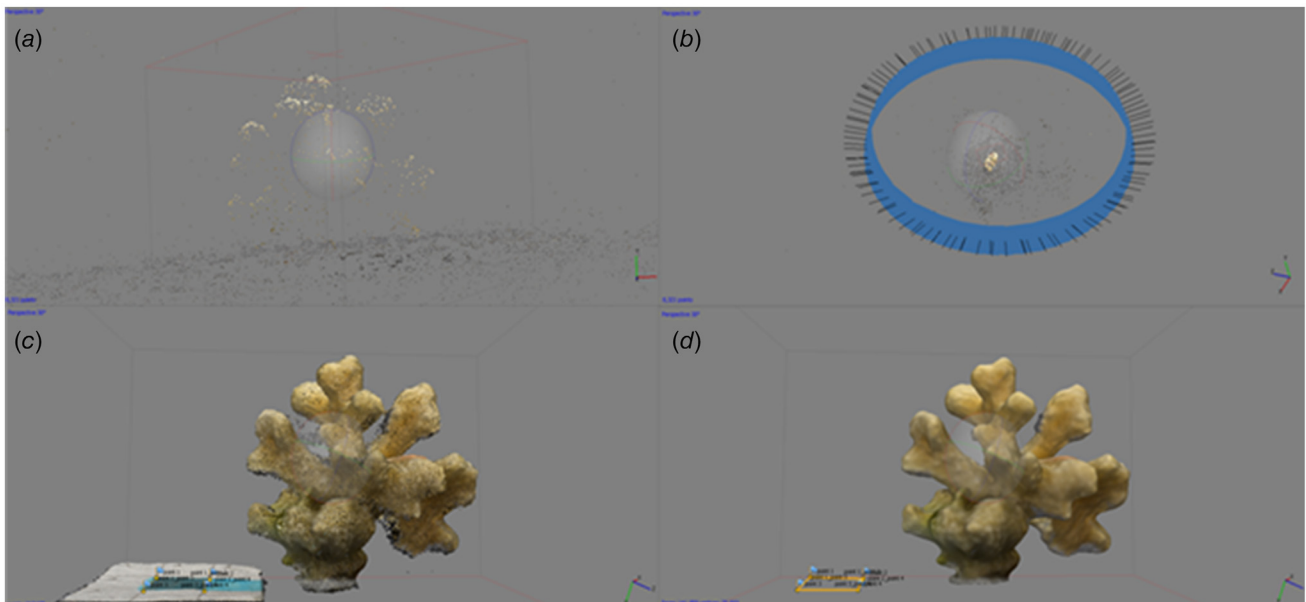


Fig. 2. Agisoft Photoscan workflow for *Stylophora pistillata*; (a) aligned points from the coral images into a three-dimensional (3-D) space; (b) alignment of pictures (in blue) and the creation of the dense point cloud; (c) creation of the high polygon mesh of the coral fragment and the scale from the dense point cloud; (d) cropped and completed 3-D model of the coral fragment, including the markers on the scale.

Prior to using 'structure from motion' photogrammetry, a preliminary evaluation was performed to compare the results of this method against the aluminium-foil method developed by Marsh (1970). Importantly, although surface-area estimates produced by both methods were statistically indistinguishable, values derived from 'structure from motion' photogrammetry exhibited the lowest mean coefficient of variation across coral fragments and as such, this was selected as our method-of-choice when normalising cell densities and Chl-*a* concentration to surface area in this study.

Macroalgal and epiphyte preparation

Macroalgae and attached epiphytic algae were cleaned and separated following an adaptation of the technique described by Zimba and Hopson (1997). Each macroalga was placed in a 200-mL screw-top jar and RO water was added until the macroalga was completely covered. The jar was closed and manually shaken for 40 s to remove the epiphytes from the macroalga. The macroalga was then removed from the jar and the epiphyte slurry, and the surface of the macroalga was visually assessed and any remaining epiphytes were carefully removed using scalpel and forceps. After removal of epiphytes, the macroalga was rinsed with RO water and oven dried for 48 h at 60°C. Each epiphyte slurry had non-algal epiphytes removed, and was then mixed and filtered through a 100- μ m mesh before baking oven-dried for 48 h at 60°C. All samples were ground to a fine powder by using a mortar and pestle, and 6–8 mg of powdered tissue was placed into a separate tin capsule for subsequent stable isotope analysis.

Stable isotope analysis

Samples were analysed for nitrogen (^{15}N : ^{14}N) and carbon (^{13}C : ^{12}C) stable isotopes by using a Europa EA GSL elemental analyser coupled to a Hydra 2022 mass spectrometer (Sercon Ltd, UK) at Griffith University (Nathan Campus, Brisbane, Qld, Australia). Precision of this spectrometer is within 0.1% for $\delta^{15}\text{N}$ and $\delta^{13}\text{C}$ values (Raoult *et al.* 2015). Ratios of ^{15}N : ^{14}N ($\delta^{15}\text{N}$) and ^{13}C : ^{12}C ($\delta^{13}\text{C}$) were expressed as the relative difference between the sample and a standard of atmospheric nitrogen (^{15}N) and Pee Dee Belemnite (^{13}C), in parts per thousand (‰). Elemental precision relative to standards was 0.2 for $\delta^{13}\text{C}$ and 0.1 for $\delta^{15}\text{N}$.

Statistical analysis

All statistical analyses were performed using RStudio (ver. 1.1.453, Posit Software, PBC, Boston, MA, USA, see <https://posit.co/>) and R (ver. 3.4.4, R Foundation for Statistical Computing, Vienna, Austria, see <https://www.r-project.org/>). First, it was necessary to determine the optimal coral surface-area measurement technique. Linear mixed models with the package *lme4* (ver. 1.8.5, see <https://CRAN.R-project.org/package=lme4>; Bates *et al.* 2015) were used to compare the

surface-area measurements obtained with structure from motion photogrammetry and the aluminium-foil method. For this analysis, surface area was the response variable and the method used was set as a fixed effect, and sites (1–10) and coral replicates (A, B, C) were treated as random effects.

ANOVA, linear regression models and paired Student's *t*-tests were used to test for differences in cell densities, *Symbiodinium*, Chl-*a* concentration and $\delta^{15}\text{N}$ and $\delta^{13}\text{C}$ values around Hideaway Island and along a depth gradient. Cell densities, Chl-*a* concentration and $\delta^{15}\text{N}$ and $\delta^{13}\text{C}$ values around the island were analysed separately by using a nested ANOVA, where zone (eastern, western, southern) around the island was treated as a fixed factor and site within each zone was treated as a random factor. To assess whether there were more specific spatial differences around the island, a one-way ANOVA where site was treated as a factor was performed for each variable. *Post hoc* Tukey HSD tests were performed if there was a significant difference across zones and sites in each analysis, by using the package *emmeans* (ver. 1.1-33, see <https://cran.r-project.org/package=emmeans>). Differences in cell densities, *Symbiodinium* Chl-*a* concentration and $\delta^{15}\text{N}$ and $\delta^{13}\text{C}$ values across a depth gradient were compared in separate linear regression analysis using the *lme4* package. Additionally, an analysis was performed comparing Chl-*a* concentration that had been standardised for surface area at different depths by using a linear regression. A paired Student's *t*-test was used to test for differences in the $\delta^{15}\text{N}$ and $\delta^{13}\text{C}$ values between macroalgae and epiphytes at each site and depth.

Results

Surface-area determination for coral

No significant difference between the measurements of coral surface area calculated from photogrammetry and the aluminium-foil method was observed ($F_{8,47} = 9.44$, $P = 0.07$). However, coral surface-area data derived from photogrammetry exhibited a lower coefficient of variation (55.5 %) than did those from the aluminium-foil method (59.6%). Therefore, the calculated area of each coral fragment determined by photogrammetry was used to normalise the Chl-*a* concentration and *Symbiodinium* density to surface area in square centimetres for all coral fragments.

Coral endosymbiont density and Chl-*a* concentration

For *M. stellata*, *Symbiodinium* cell densities ($F_{2,7} = 5.53$, $P = 0.03$; Fig. 3a) and Chl-*a* concentration ($F_{2,7} = 4.72$, $P = 0.05$; Fig. 3b) were significantly different among the three zones. Samples collected at the southern zone had the highest Chl-*a* concentration in *Symbiodinium*, as well as the

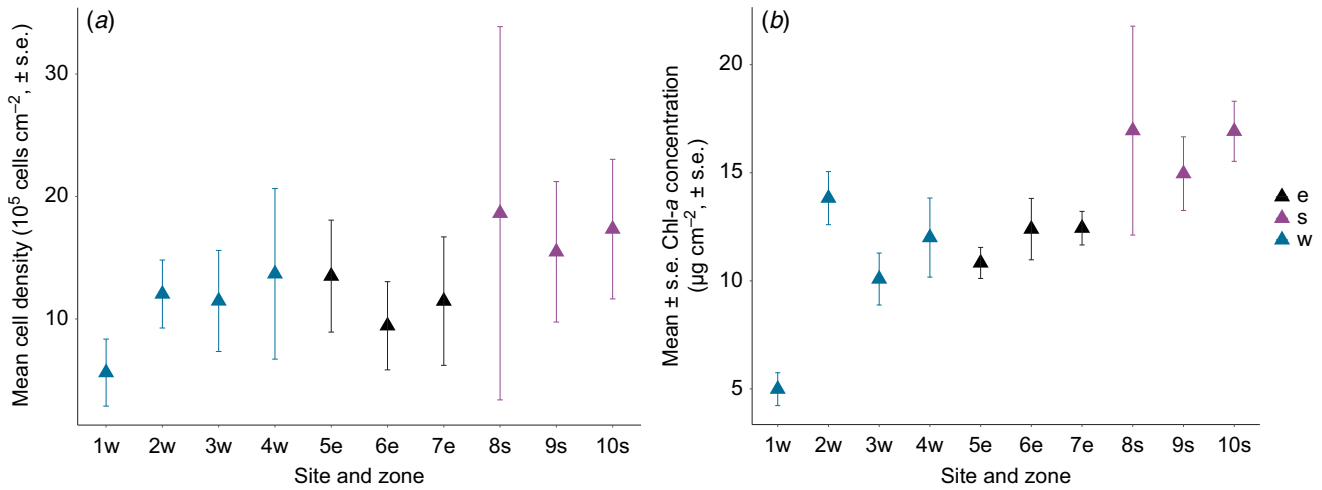


Fig. 3. Mean (± 1 s.e.) (a) cell density (10⁵ cells cm⁻²) and (b) Chl-a concentration (µg cm⁻²) of *Symbiodinium* from *Montipora stellata* at 10 sites around Hideaway Island. Zones in relation to the island are denoted by: w, western; e, eastern; s, southern.

Table 1. Mean (± 1 s.e.) cell densities and chlorophyll-a (Chl-a) concentration of *Symbiodinium* from *Montipora stellata*, from the three zones (eastern, western, southern) around Hideaway Island.

Zone	Cell density (10 ⁵ cells cm ⁻²)	Chl-a concentration (µg cm ⁻²)
Eastern	11.46 ± 0.94	11.88 ± 0.58
Western	10.70 ± 0.91	10.22 ± 0.92
Southern	17.15 ± 1.19	16.27 ± 1.67

highest average cell density compared with the western and eastern zones (Table 1).

Cell densities and Chl-a concentration of *Symbiodinium* from *S. pistillata* differed in their responses to depth ($F_{1,37} = 14.64$, $P < 0.001$, $R^2 = 0.26$). *Symbiodinium* cell density decreased significantly as depth increased ($F_{1,37} = 10.38$, $P < 0.001$, $R^2 = 0.12$; Fig. 4a); however, surface area-normalised Chl-a

concentration remained unchanged with depth ($F_{1,37} = 2.06$, $P = 0.15$, $R^2 = 0.03$; Fig. 4b).

Spatial changes in the nutrient signatures of primary producers

The δ¹⁵N mean values for *Symbiodinium* from *M. stellata* did not differ significantly among the three zones however, significant differences were observed at the site level (Table 1; $F_{9,16} = 21.49$, $P < 0.01$). Specifically, *Symbiodinium* δ¹⁵N values from Site 1 in the western zone were higher than those from the remaining of the nine sites ($P < 0.01$). The majority of macroalgae collected from each site had epiphytic algae attached. No significant differences in δ¹⁵N values of macroalgae and epiphytes were observed among the three zones (Table 2); however, nutrient signatures were much more variable for both macroalgae and epiphytic algae than for the endosymbiotic algae. However, significant differences in

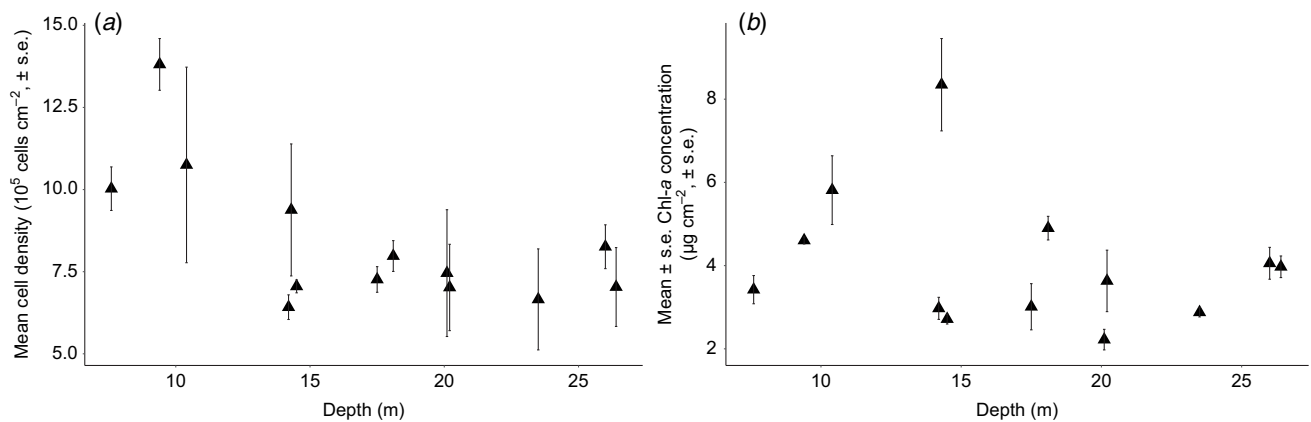


Fig. 4. Mean (± 1 s.e.) (a) cell densities (10⁵ cells cm⁻²), and (b) chlorophyll-a (Chl-a) concentration (µg cm⁻²) of *Symbiodinium* from *Stylophora pistillata* along a depth gradient.

Table 2. Values (mean \pm s.e.) of $\delta^{15}\text{N}$ and $\delta^{13}\text{C}$ of *Symbiodinium* from *Montipora stellata*, macroalgae (mix of *Actinotrichia fragilis* and *Galaxaura rugosa*) and epiphytes from the three zones (eastern, western, southern) around Hideaway Island.

Zone	$\delta^{15}\text{N}\%$ <i>Symbiodinium</i>	$\delta^{15}\text{N}\%$ macroalgae	$\delta^{15}\text{N}\%$ epiphytes	$\delta^{13}\text{C}\%$ <i>Symbiodinium</i>	$\delta^{13}\text{C}\%$ macroalgae	$\delta^{13}\text{C}\%$ epiphytes
Eastern	4.1 \pm 0.1	6.4 \pm 0.6	2.3 \pm 0.2	-14.0 \pm 0.2	-9.9 \pm 0.3	-13.4 \pm 0.7
Western	4.4 \pm 0.1	5.1 \pm 0.6	2.7 \pm 0.3	-13.8 \pm 0.1	-9.1 \pm 0.3	-14.4 \pm 0.7
Southern	4.2 \pm 0.1	6.0 \pm 0.4	3.4 \pm 0.3	-14.4 \pm 0.1	-10.1 \pm 0.2	-13.7 \pm 1.0

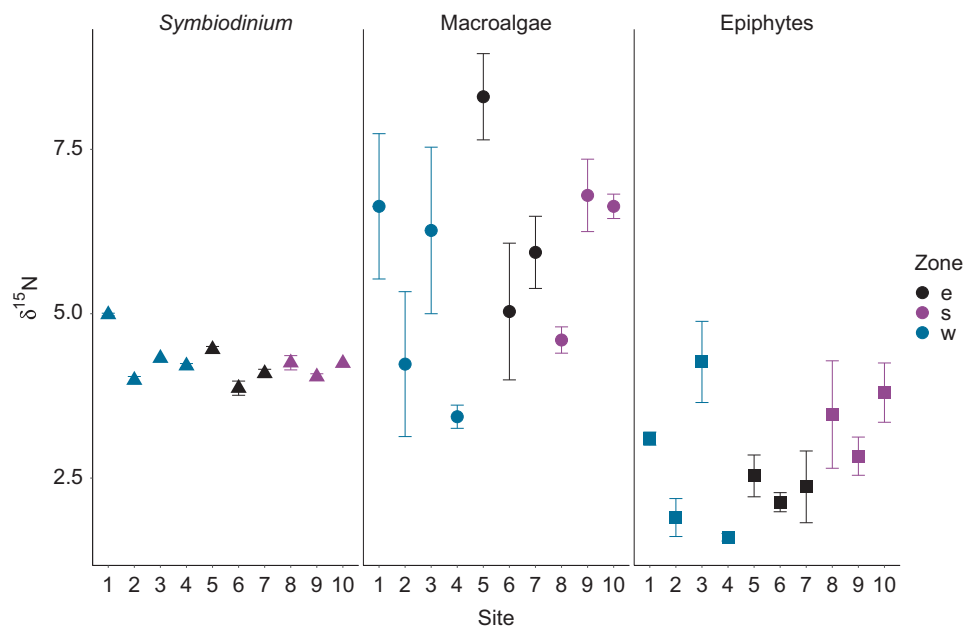
macroalgal $\delta^{15}\text{N}$ values were detected when the 10 sites around the island were analysed independently regardless of zone ($F_{9,20} = 3.36$, $P = 0.01$). Specifically, the $\delta^{15}\text{N}$ values of macroalgae from Site 5 in the eastern zone were significantly higher than those from Sites 2 ($P = 0.04$) and 4 ($P < 0.01$) within the western zone (Fig. 5). Overall, $\delta^{15}\text{N}$ values of epiphytes were lower than those of the macroalgae (Table 2).

Significant differences were detected between $\delta^{13}\text{C}$ values of *Symbiodinium* ($F_{2,23} = 3.77$, $P = 0.03$) among the three zones around Hideaway Island (Fig. 6). *Symbiodinium* individuals from the western zone were significantly more enriched than those from the southern zone ($P = 0.01$). However, the $\delta^{13}\text{C}$ values of *Symbiodinium* from the southern and eastern zones were similar (*post hoc* Tukey $P > 0.1$), together with the eastern and western zones ($P > 0.5$). The mean $\delta^{13}\text{C}$ values of macroalgae and epiphytes collected at the three different zones around Hideaway Island at the same depth exhibited no differences among the zones, but were highly variable within a site (Fig. 6). Overall, the macroalgae collected around the island displayed the highest $\delta^{13}\text{C}$

values compared with those of *Symbiodinium* and epiphytes (Table 2).

Depth changes in the nutrient signatures of primary producers

Values of $\delta^{15}\text{N}$ for *Symbiodinium* from *S. pistillata* ranged from 3.9‰ at 23.5-m depth to 5.2‰ at 26-m depth (Fig. 7). No significant influence of depth was observed for $\delta^{15}\text{N}$ from *Symbiodinium* ($F_{1,9} = 1.59$, $P = 0.23$). $\delta^{15}\text{N}$ values for macroalgae ranged from 2.8‰ at 15.8-m depth to 4.8‰ at 6.6-m depth. $\delta^{15}\text{N}$ values for epiphytes varied along the depth gradient, with the lowest $\delta^{15}\text{N}$ value of 2.6‰ at 13.6- and 17-m depth, and the highest value of 4.6‰ at 23-m depth (Fig. 7). No influence of depth on the $\delta^{15}\text{N}$ values of macroalgae ($F_{1,15} = 0.67$, $P = 0.43$) or epiphytes ($F_{1,18} = 1.23$, $P = 0.28$) was observed. No significant differences were observed between the mean $\delta^{15}\text{N}$ values of the macroalgae and the epiphytic algae ($P = 0.61$). Overall, $\delta^{15}\text{N}$ values of *Symbiodinium* were higher than those of the macroalgae and epiphytes.

**Fig. 5.** Values (mean \pm s.e.) of $\delta^{15}\text{N}$ of *Symbiodinium* from *Montipora stellata*, macroalgae, and epiphytes around Hideaway Island. Zones in relation to the island are denoted by: w, western; e, eastern; s southern.

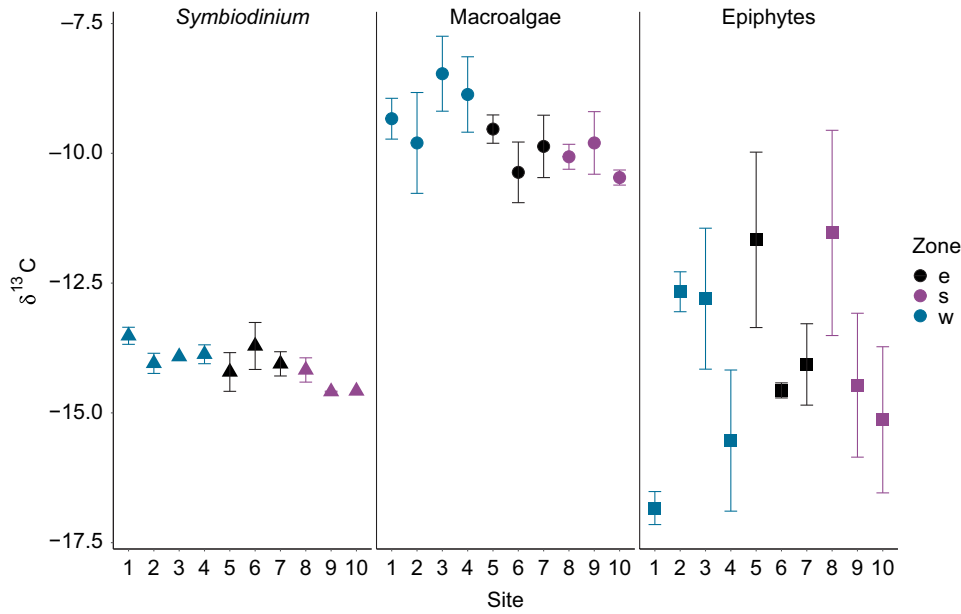


Fig. 6. Values (mean ± s.e.) of $\delta^{13}\text{C}$ of *Symbiodinium* from *Montipora stellata*, macroalgae, and epiphytes around Hideaway Island. Zones in relation to the island are denoted by: w, western; e, eastern; s, southern.

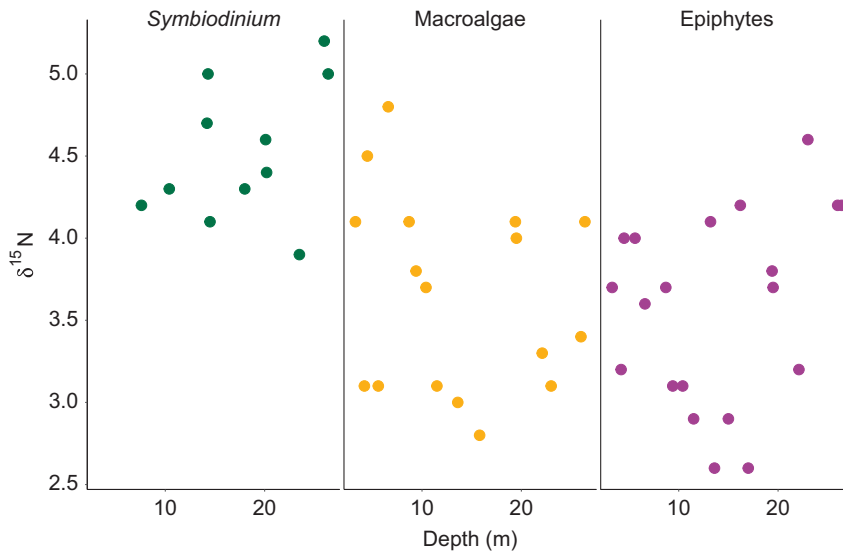


Fig. 7. Variability of $\delta^{15}\text{N}$ values of *Symbiodinium* from *Stylophora pistillata*, macroalgae and epiphytes along a depth gradient from 3 to 26 m.

Depth had a significant influence on the $\delta^{13}\text{C}$ values for macroalgae, but not for the epiphytes or *Symbiodinium*. $\delta^{13}\text{C}$ values of *Symbiodinium* from *S. pistillata* ranged from -18‰ at 14.3-m depth to -15.2‰ at 10.4-m depth. $\delta^{13}\text{C}$ values of *Symbiodinium* exhibited no differences across depth ($F_{1,11} = 1.81, P = 0.21, R^2 = 0.06$). $\delta^{13}\text{C}$ values of macroalgae ranged from -20.3‰ at 19.4-m depth to -4.2‰ at 17-m depth, whereas $\delta^{13}\text{C}$ values of the epiphytes ranged from -24.8‰ at 26.4-m depth to -6.1‰ at 22.1-m depth. $\delta^{13}\text{C}$ values differed significantly ($P < 0.001$) between the macroalgae and epiphytes along the depth gradient. Macroalgal $\delta^{13}\text{C}$

values were higher than the epiphyte $\delta^{13}\text{C}$ values, and both displayed high variability in values along the depth gradient (Fig. 8). $\delta^{13}\text{C}$ values of macroalgae varied significantly with depth ($F_{1,22} = 15.47, P < 0.001, R^2 = 0.39$), whereas no influence of depth was observed in $\delta^{13}\text{C}$ values of the epiphytes ($F_{1,18} = 2.3, P = 0.15, R^2 = 0.06$). Macroalgal samples collected at depths of less than 20 m displayed $\delta^{13}\text{C}$ values up to -10‰ , and those collected at depths deeper than 20 m displayed values lower than -10‰ . Overall, the $\delta^{13}\text{C}$ values of *Symbiodinium* from *S. pistillata* were more depleted than the $\delta^{13}\text{C}$ values of macroalgae and epiphytes

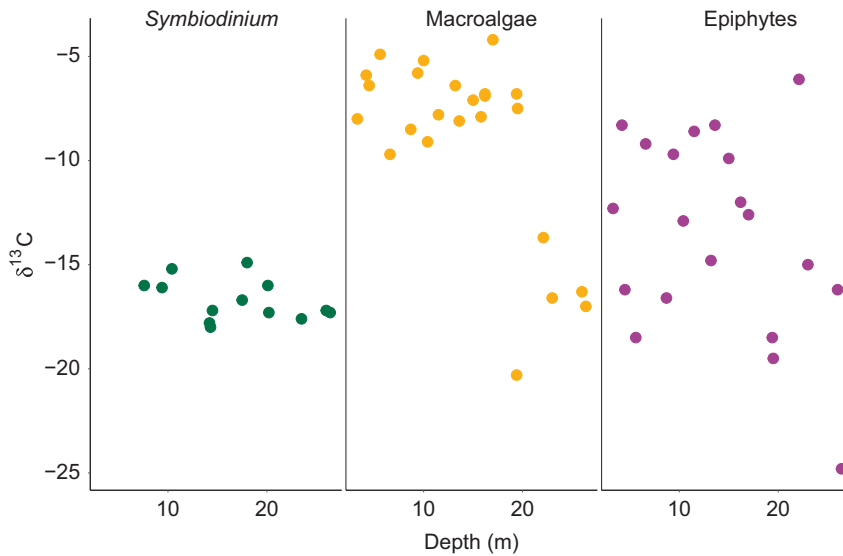


Fig. 8. Variability of $\delta^{13}\text{C}$ values of *Symbiodinium* from *Stylophora pistillata*, macroalgae and epiphytes along a depth gradient from 3 to 26 m.

and displayed lower variability along the depth gradient (Fig. 8).

Discussion

This study examined the nutrient profiles of primary producers on a coral reef flat at a spatial scale and examined the influence of depth on the basis of the function of the producers. The results presented here provide a preliminary baseline for future studies that analyse N and C stable isotopes in benthic primary producers, both at this location, and on similar reef flats. Such baselines provide a useful benchmark tool for assessing anthropogenic pollution, tracking nutrient sources and waste management, and understanding how the relationship among photosynthetic, nutrient and carbon pathways in coral reefs may be affected by future climate change.

Spatial changes in the nutrient signatures of primary producers

Although clear nutrient profiles could be obtained for *Symbiodinium*, macroalgae and epiphytic algae, none of these functional groups of primary producers showed clear spatial patterns of nutrient signatures for nitrogen or carbon at the zonal or site resolution in our study. As such, we were unable to demonstrate that stable isotope analyses can be used to detect spatial changes in primary producers in a lagoonal reef at the scale of this study. However, several factors that could account for this result. Notably, sampling was conducted at a medium scale (i.e. <1 km) around a small island and at only a single point in time, noting that nutrient availability can differ seasonally in coral reef environments (Hatcher 1990). Clearly, a more comprehensive

and extensive study that measures nutrients in the surrounding water, in addition to the nutrient profiles of the primary producers, is warranted, ideally encompassing additional locations across multiple time scales so as to properly tease apart the various factors at play.

Variability of nutrient signatures differed among samples collected within sites for macroalgae and epiphytic algae, as observed in the large standard errors at each site. Moreover, generally both carbon and nitrogen values were higher for macroalgae than for epiphytes. Such variances may have been a result of species-specific nutrient profiles; however, the different nutrient values among sites suggest otherwise. Biotic interactions between benthic marine macroalgae and other organisms are quite broad (Hurd *et al.* 2014). Most of the macroalgae collected around Hideaway Island had epiphytic algae attached, yet macroalgae displayed more enriched $\delta^{15}\text{N}$ values than did their attached epiphytes. This appears to contradict previous work that suggests that macroalgae usually exhibit a decreased nutrient profile, owing to the fact that epiphytes can access and utilise nutrients before macroalgae, and further exacerbate the issue by shading macroalgal tissue and thus restricting light availability, as observed in Wright *et al.* (2000) in temperate regions. Further research assessing macroalgae and epiphytic algae at a species level rather than a functional level would be beneficial.

$\delta^{15}\text{N}$ values of *Symbiodinium* from *M. stellata* were substantially less variable at the site scale than were those of macroalgae and epiphytes. This observation supports the hypothesis that macroalgae and epiphytes may be obtaining nitrogen directly from the water column and, thus, may be susceptible to the vagaries of variable exogenous nutrient supply (Umezawa *et al.* 2002), whereas the endosymbiotic algae can source nitrogen through nutrient-recycling within the coral host, in addition to obtaining it directly from the

environment (Grottoli et al. 2006). Interestingly, $\delta^{15}\text{N}$ values for *Symbiodinium* (3.9–5‰) in our study were similar to those reported for endosymbiotic algae in coral reef environments lacking anthropogenic nitrogen sources, such as in Dongsha Atoll, Taiwan 4.7‰ (Wong et al. 2017). The $\delta^{15}\text{N}$ range of macroalgae in this study (2.8–8.8‰) was also lower than that previously reported for macroalgae that utilise sewage as a nutrient source, namely +8.5‰ (Lapointe et al. 2005), or +9‰ (Costanzo et al. 2001). These results suggest that no anthropogenic nutrient source was present that could be detected in the $\delta^{15}\text{N}$ values of benthic primary producers around Hideaway Island at the time of sampling. However, nutrient content in the waters from the river sources and around Hideaway Island need to be directly measured for nitrates, phosphates and faecal coliforms to fully determine the nature and extent of anthropogenic nutrient loading in this ecosystem.

Carbon SIA can be used as a tool to distinguish autotrophic and heterotrophic sources (Seemann 2013). $\delta^{13}\text{C}$ values of *Symbiodinium* from *M. stellata* in this study (–13.1 to –14.7‰) were in a range similar to those previously reported for several symbiotic corals of –10 to –13‰ (Muscatine et al. 1989), –10 to –16‰ (Risk et al. 1994), and –12 to –14‰ (Swart et al. 2005). These previous studies attributed this range of $\delta^{13}\text{C}$ values to autotrophy in endosymbiotic algae obtaining recycled carbon sources from their hosts. The narrow range of $\delta^{13}\text{C}$ values of *Symbiodinium* observed here similarly indicates that the carbon sources are being recycled from the coral host.

Carbon stable isotope values in macroalgae are primarily associated with photosynthetic pathways (Cloern et al. 2002), which often exhibit great diversity across macroalgal lineages (e.g. Zweng et al. 2018). As a result, differences in macroalgal $\delta^{13}\text{C}$ values vary with species. Green algae are usually more ^{13}C enriched (–12‰) than are red algae (–18.3‰) (Yamamuro et al. 1995; Wang and Yeh 2003). As with nitrogen, therefore, differences in macroalgal and epiphytic algal $\delta^{13}\text{C}$ observed in this study may be attributed to species-specific differences in carbon sources. $\delta^{13}\text{C}$ values of macroalgae had a narrower range and were more enriched (–7.6 to –11.1‰) than those of epiphytic algae (–8.3 to –17.8‰) in our study, displaying trends similar to those previously reported (Jaschinski et al. 2008; Zheng et al. 2015). The more positive $\delta^{13}\text{C}$ values observed in the macroalgal samples suggest that macroalgae may rely more on HCO_3^- as a nutrient source, whereas the more negative $\delta^{13}\text{C}$ values observed in epiphytic algae suggest that their main carbon source may be CO_2 . This affinity of carbon sources may be the reason for the observed differences in $\delta^{13}\text{C}$ values in the macroalgae and epiphytic algae, but it needs to be empirically tested.

Depth changes in the nutrient signatures of primary producers

Depth had a significant effect on the nitrogen and carbon profiles for macroalgae, but not for either epiphytic algae

or endosymbiotic algae. Concentrations of both nitrogen and carbon decreased with an increasing depth in macroalgae. High variability of nitrogen and carbon was observed for macroalgae and epiphytes and this, coupled with a lack of replication of depth profiles, makes it difficult to infer any causal relationships here. Similar to our results, previous macroalgal studies have found no clear pattern in these values that could correlate to depth or taxonomy of the species (Marconi et al. 2011).

Depletions in nitrogen and carbon isotopes with increasing depths at Hideaway Island could be attributed to a reduced rate of photosynthesis as a result of reduced light availability. It has been previously reported that macroalgal species with $\delta^{13}\text{C}$ values more enriched than –10‰ use HCO_3^- as a carbon source (Raven 1997). Therefore, we suggest that our macroalgae collected at waters 3–20 m deep with $\delta^{13}\text{C}$ values of –4.2 to –10‰ may have also been using HCO_3^- as a carbon source, whereas macroalgae in deeper waters (below 20 m depth) may have been using dissolved CO_2 , which has more depleted $\delta^{13}\text{C}$ values (Raven 1997). $\delta^{13}\text{C}$ values in macroalgae in this study suggest that at shallow depths, macroalgae have higher photosynthetic rates than, and utilise a different carbon source from macroalgae from deeper waters. This suggests that macroalgae in our study were relying on photosynthesis for nutrient production.

The variability in cell density and Chl-*a* concentration decreased for samples collected in depths of 15 m or greater for *Symbiodinium* from *S. pistillata* in our study. These results align with previous research that has shown that *S. pistillata* increases its photosynthetic activity at depth to compensate for the decrease in light, to satisfy the nutritional budgets of the coral host (e.g. Mass et al. 2007). However, contrary to our results, other studies have reported a corresponding increase in Chl-*a* concentration for *Symbiodinium* from *S. pistillata* as depth increases to 30 m (Gattuso et al. 1993). While more research is required to understand why Chl-*a* concentration did not appear to increase with depth in our study, and the ubiquity of our results in terms of other depth profiles and reefs, our results, nevertheless, remain a useful baseline for future research in this region.

$\delta^{15}\text{N}$ values of *Symbiodinium* from *S. pistillata* remained consistent over the depth gradient. This indicates that any changes in the isotopic composition of coral tissues over depth may be driven by increased heterotrophy as corals reduce their reliance on photosynthesis. Grottoli et al. (2006) found that different species of coral differ in their trophic plasticity depending on environmental factors such as depth, light, and nutrient availability. $\delta^{15}\text{N}$ values obtained for *Symbiodinium* here were higher than those previously reported for *S. pistillata* endosymbionts, but followed the same trend of no enrichment with an increasing depth (Alamaru et al. 2009). This could be explained by different $\delta^{15}\text{N}$ values of inorganic nitrogen sources present, although this was not explicitly tested in our study. Further studies should increase the depth range at which corals are collected and assess the

nitrogen and carbon isotopic composition of sympatric symbiotic corals to determine whether the patterns observed here apply to all endosymbionts.

Symbiodinium $\delta^{13}\text{C}$ values in this study did not show a decrease with an increasing depth. Our results support previous studies where no significant depletion in the $\delta^{13}\text{C}$ of *Symbiodinium* was observed above 30-m depth (Einbinder *et al.* 2009). Although previous studies have documented depletions in the $\delta^{13}\text{C}$ values of *Symbiodinium* and coral tissue with an increasing depth (Muscatine *et al.* 1989; Alamaru *et al.* 2009), the observed depletion trends were significant only from 15- to 60-m depth. The constant $\delta^{13}\text{C}$ values of *Symbiodinium* from *S. pistillata* along the depth gradient align with the concept of recycling carbon sources between the coral host and its symbionts (Reynaud *et al.* 2009). Alternatively, a high rate of carbon and nitrogen recycling between the coral host and *Symbiodinium* may occur as depth increases, which could result in lower isotopic fractionation (Einbinder *et al.* 2009). *Symbiodinium* may have been using CO_2 from the coral host for photosynthesis rather than externally available carbon sources in our study. We conclude that depleted and constant $\delta^{13}\text{C}$ values of *Symbiodinium* suggest that the carbon source might be sourced from both photosynthesis and the coral host.

Implications

Our research is one of the first studies to successfully show that SIA can be used to detect changes in nitrogen and carbon signatures for primary producers to discern between functional roles on shallow tropical reefs. Although this study was small in scope, its uniqueness sets the scene for future, more comprehensive research on detection of carbon and nitrogen nutritional signatures on primary producers in coral reefs more broadly. Understanding the origins of such nutrients on coral reefs and how uptake may vary in relation to nutrient availability and environmental factors may be key in understanding drivers behind bright and dark spots on coral reefs (Cinner *et al.* 2016).

References

- Alamaru A, Loya Y, Brokovich E, Yam R, Shemesh A (2009) Carbon and nitrogen utilization in two species of Red Sea corals along a depth gradient: insights from stable isotope analysis of total organic material and lipids. *Geochimica et Cosmochimica Acta* 73(18), 5333–5342. doi:10.1016/j.gca.2009.06.018
- Anthony KRN, Fabricius KE (2000) Shifting roles of heterotrophy and autotrophy in coral energetics under varying turbidity. *Journal of Experimental Marine Biology and Ecology* 252(2), 221–253. doi:10.1016/S0022-0981(00)00237-9
- Baker AC (2003) Flexibility and specificity in coral-algal symbiosis: diversity, ecology, and biogeography of *Symbiodinium*. *Annual Review of Ecology, Evolution, and Systematics* 34(1), 661–689. doi:10.1146/annurev.ecolsys.34.011802.132417
- Bates D, Mächler M, Bolker B, Walker S (2015) Fitting linear mixed-effects models using lme4. *Journal of Statistical Software* 67(1), 1–48. doi:10.18637/jss.v067.i01
- Baums IB, Baker AC, Davies SW, Grottoli AG, Kenkel CD, Kitchen SA, Kuffner IB, LaJeunesse TC, Matz MV, Miller MW, Parkinson JE, Shantz AA (2019) Considerations for maximizing the adaptive potential of restored coral populations in the western Atlantic. *Ecological Applications* 29(8), e01978. doi:10.1002/eap.1978
- Brandl SJ, Rasher DB, Côté IM, Casey JM, Darling ES, Lefcheck JS, Duffy JE (2019) Coral reef ecosystem functioning: eight core processes and the role of biodiversity. *Frontiers in Ecology and the Environment* 17(8), 445–454. doi:10.1002/fee.2088
- Buckwell A, Ware D, Fleming C, Smart JCR, Mackey B, Nalau J, Dan A (2020) Social benefit cost analysis of ecosystem-based climate change adaptations: a community-level case study in Tanna Island, Vanuatu. *Climate and Development* 12(6), 495–510. doi:10.1080/17565529.2019.1642179
- Burke LM, Reyta K, Spalding M, Perry A (2012) 'Reefs at risk revisited in the coral triangle.' (World Resources Institute)
- Carricart-Ganivet JP, Beltrán-Torres AU, Merino M, Ruiz-Zárata MA (2000) Skeletal extension, density and calcification rate of the reef building coral *Montastraea annularis* (Ellis and Solander) in the Mexican Caribbean. *Bulletin of Marine Science* 66(1), 215–224.
- Chan NCS, Wangpraseurt D, Kühl M, Connolly SR (2016) Flow and coral morphology control coral surface pH: implications for the effects of ocean acidification. *Frontiers in Marine Science* 3, 10. doi:10.3389/fmars.2016.00010
- Cinner JE, Huchery C, MacNeil MA, Graham NAJ, McClanahan TR, Maina J, Maire E, Kittinger JN, Hicks CC, Mora C, Allison EH, D'Agata S, Hoey A, Feary DA, Crowder L, Williams ID, Kulbicki M, Vigliola L, Wantiez L, Edgar G, Stuart-Smith RD, Sandin SA, Green AL, Hardt MJ, Beger M, Friedlander A, Campbell SJ, Holmes KE, Wilson SK, Brokovich E, Brooks AJ, Cruz-Motta JJ, Booth DJ, Chabanet P, Gough C, Tupper M, Ferse SCA, Sumaila UR, Mouillot D (2016) Bright spots among the world's coral reefs. *Nature* 535(7612), 416–419. doi:10.1038/nature18607
- Cloern JE, Canuel EA, Harris D (2002) Stable carbon and nitrogen isotope composition of aquatic and terrestrial plants of the San Francisco Bay estuarine system. *Limnology and Oceanography* 47(3), 713–729. doi:10.4319/lo.2002.47.3.0713
- Costanzo SD, O'donohue MJ, Dennison WC, Loneragan NR, Thomas M (2001) A new approach for detecting and mapping sewage impacts. *Marine Pollution Bulletin* 42(2), 149–156. doi:10.1016/S0025-326X(00)00125-9
- Einbinder S, Mass T, Brokovich E, Dubinsky Z, Erez J, Tchernov D (2009) Changes in morphology and diet of the coral *Stylophora pistillata* along a depth gradient. *Marine Ecology Progress Series* 381, 167–174. doi:10.3354/meps07908
- Eurich JG, Matley JK, Baker R, McCormick MI, Jones GP (2019) Stable isotope analysis reveals trophic diversity and partitioning in territorial damselfishes on a low-latitude coral reef. *Marine Biology* 166(2), 17. doi:10.1007/s00227-018-3463-3
- Ezzat L, Fine M, Maguer J-F, Grover R, Ferrier-Pagès C (2017) Carbon and nitrogen acquisition in shallow and deep holobionts of the scleractinian coral *S. pistillata*. *Frontiers in Marine Science* 4, 102. doi:10.3389/fmars.2017.00102
- Fabricius KE (2005) Effects of terrestrial runoff on the ecology of corals and coral reefs: review and synthesis. *Marine Pollution Bulletin* 50(2), 125–146. doi:10.1016/j.marpolbul.2004.11.028
- Fry B, Sherr EB (1989) $\delta^{13}\text{C}$ measurements as indicators of carbon flow in marine and freshwater ecosystems. In 'Stable isotopes in ecological research'. (Eds PW Rundel, JR Ehleringer, KA Nagy) pp. 196–229. (Springer)
- Gattuso J-P, Yellowlees D, Lesser M (1993) Depth- and light-dependent variation of carbon partitioning and utilization in the zooxanthellate scleractinian coral *Stylophora pistillata*. *Marine Ecology Progress Series* 92 (3), 267–276. doi:10.3354/meps092267
- Grottoli AG, Rodrigues LJ, Juarez C (2004) Lipids and stable carbon isotopes in two species of Hawaiian corals, *Porites compressa* and *Montipora verrucosa*, following a bleaching event. *Marine Biology* 145(3), 621–631. doi:10.1007/s00227-004-1337-3
- Grottoli AG, Rodrigues LJ, Palardy JE (2006) Heterotrophic plasticity and resilience in bleached corals. *Nature* 440(7088), 1186–1189. doi:10.1038/nature04565

- Hatcher BG (1990) Coral reef primary productivity. A hierarchy of pattern and process. *Trends in Ecology & Evolution* 5(5), 149–155. doi:10.1016/0169-5347(90)90221-X
- Hoegh-Guldberg O, Williamson J (1999) Availability of two forms of dissolved nitrogen to the coral *Pocillopora damicornis* and its symbiotic zooxanthellae. *Marine Biology* 133(3), 561–570. doi:10.1007/s002270050496
- Hoey AS, Howells E, Johansen JL, Hobbs J-PA, Messmer V, McCowan DM, Wilson SK, Pratchett MS (2016) Recent advances in understanding the effects of climate change on coral reefs. *Diversity* 8(4), 12. doi:10.3390/d8020012
- House JE, Brambilla V, Bidaut LM, Christie AP, Pizarro O, Madin JS, Dornelas M (2018) Moving to 3D: relationships between coral planar area, surface area and volume. *PeerJ* 6, e4280. doi:10.7717/peerj.4280
- Hurd CL, Harrison PJ, Bischof K, Lobban CS (2014) 'Seaweed ecology and physiology.' (Cambridge University Press)
- Jaschinski S, Brepohl DC, Sommer U (2008) Carbon sources and trophic structure in an eelgrass *Zostera marina* bed, based on stable isotope and fatty acid analyses. *Marine Ecology Progress Series* 358, 103–114. doi:10.3354/meps07327
- Jeffrey SW, Humphrey GF (1975) New spectrophotometric equations for determining chlorophylls *a*, *b*, *c1* and *c2* in higher plants, algae and natural phytoplankton. *Biochimie und Physiologie der Pflanzen* 167(2), 191–194. doi:10.1016/S0015-3796(17)30778-3
- Johnson MD, Fox MD, Kelly ELA, Zgliczynski BJ, Sandin SA, Smith JE (2020) Ecophysiology of coral reef primary producers across an upwelling gradient in the tropical central Pacific. *PLoS ONE* 15(2), e0228448. doi:10.1371/journal.pone.0228448
- Koop K, Booth D, Broadbent A, Brodie J, Bucher D, Capone D, Coll J, Dennison W, Erdmann M, Harrison P, Hoegh-Guldberg O, Hutchings P, Jones GB, Larkum AWD, O'Neil J, Steven A, Tentori E, Ward S, Williamson J, Yellowlees D (2001) ENCORE: the effect of nutrient enrichment on coral reefs. Synthesis of results and conclusions. *Marine Pollution Bulletin* 42(2), 91–120. doi:10.1016/S0025-326X(00)00181-8
- Kowec DA, Forden A, Albright R, Takeshita Y, Mucciarone DA, Ninokawa A, Caldeira K (2019) Carbon isotopic fractionation in organic matter production consistent with benthic community composition across a coral reef flat. *Frontiers in Marine Science* 5, 520. doi:10.3389/fmars.2018.00520
- Lapointe BE (1997) Nutrient thresholds for bottom-up control of macroalgal blooms on coral reefs in Jamaica and southeast Florida. *Limnology and Oceanography* 42(5part2), 1119–1131. doi:10.4319/lo.1997.42.5_part_2.1119
- Lapointe BE, Barile PJ, Littler MM, Littler DS (2005) Macroalgal blooms on southeast Florida coral reefs: II. Cross-shelf discrimination of nitrogen sources indicates widespread assimilation of sewage nitrogen. *Harmful Algae* 4(6), 1106–1122. doi:10.1016/j.hal.2005.06.002
- Lesser MP, Slattery M, Stat M, Ojimi M, Gates RD, Grottolli A (2010) Photoacclimatization by the coral *Montastraea cavernosa* in the mesophotic zone: light, food, and genetics. *Ecology* 91(4), 990–1003. doi:10.1890/09-0313.1
- Marconi M, Giordano M, Raven JA (2011) Impact of taxonomy, geography, and depth on $\delta^{13}\text{C}$ and $\delta^{15}\text{N}$ variation in a large collection of macroalgae. *Journal of Phycology* 47(5), 1023–1035. doi:10.1111/j.1529-8817.2011.01045.x
- Marsh JA Jr. (1970) Primary productivity of reef-building calcareous red algae. *Ecology* 51(2), 255–263. doi:10.2307/1933661
- Mass T, Einbinder S, Brokovich E, Shashar N, Vago R, Erez J, Dubinsky Z (2007) Photoacclimation of *Stylophora pistillata* to light extremes: metabolism and calcification. *Marine Ecology Progress Series* 334, 93–102. doi:10.3354/meps334093
- McMahon KW, Thorrold SR, Houghton LA, Berumen ML (2016) Tracing carbon flow through coral reef food webs using a compound-specific stable isotope approach. *Oecologia* 180(3), 809–821. doi:10.1007/s00442-015-3475-3
- Mollica NR, Guo W, Cohen AL, Huang K-F, Foster GL, Donald HK, Solow AR (2018) Ocean acidification affects coral growth by reducing skeletal density. *Proceedings of the National Academy of Sciences* 115(8), 1754–1759. doi:10.1073/pnas.1712806115
- Mosley LM, Aalbersberg WGL (2003) Nutrient levels in sea and river water along the 'coral coast' of Viti Levu, Fiji. *The South Pacific Journal of Natural and Applied Sciences* 21(1), 35–40. doi:10.1071/SP03007
- Muscantine L, Porter JW, Kaplan IR (1989) Resource partitioning by reef corals as determined from stable isotope composition. I. $\delta^{13}\text{C}$ of zooxanthellae and animal tissue vs depth. *Marine Biology* 100(2), 185–193. doi:10.1007/BF00391957
- Muscantine L, Goiran C, Land L, Jaubert J, Cuif J-P, Allemand D (2005) Stable isotopes ($\delta^{13}\text{C}$ and $\delta^{15}\text{N}$) of organic matrix from coral skeleton. *Proceedings of the National Academy of Sciences of the United States of America* 102(5), 1525–1530. doi:10.1073/pnas.0408921102
- Owens NJP (1988) Natural variations in ^{15}N in the marine environment. *Advances in Marine Biology* 24, 389–451. doi:10.1016/S0065-2881(08)60077-2
- Perry CT, Kench PS, Smithers SG, Riegl B, Yamano H, O'Leary MJ (2011) Implications of reef ecosystem change for the stability and maintenance of coral reef islands. *Global Change Biology* 17(12), 3679–3696. doi:10.1111/j.1365-2486.2011.02523.x
- Poustie MS, Deletic A (2014) Modeling integrated urban water systems in developing countries: case study of Port Vila, Vanuatu. *AMBIO* 43(8), 1093–1111. doi:10.1007/s13280-014-0538-3
- Raoult V, Gaston TF, Williamson JE (2015) Not all sawsharks are equal: species of co-existing sawsharks show plasticity in trophic consumption both within and between species. *Canadian Journal of Fisheries and Aquatic Sciences* 72(11), 1769–1775. doi:10.1139/cjfas-2015-0307
- Raoult V, Reid-Anderson S, Ferri A, Williamson JE (2017) How reliable is structure from motion (SfM) over time and between observers? A case study using coral reef bommies. *Remote Sensing* 9(7), 740. doi:10.3390/rs9070740
- Raven JA (1997) Inorganic carbon acquisition by marine autotrophs. *Advances in Botanical Research* 27, 85–209. doi:10.1016/S0065-2296(08)60281-5
- Reynaud S, Martinez P, Houlbrèque F, Billy I, Allemand D, Ferrier-Pagès C (2009) Effect of light and feeding on the nitrogen isotopic composition of a zooxanthellate coral: role of nitrogen recycling. *Marine Ecology Progress Series* 392, 103–110. doi:10.3354/meps08195
- Risk MJ, Sammarco PW, Schwarcz HP (1994) Cross-continental shelf trends in $\delta^{13}\text{C}$ in coral on the Great Barrier Reef. *Marine Ecology Progress Series* 106, 121–130. doi:10.3354/meps106121
- Risk MJ, Lapointe BE, Sherwood OA, Bedford BJ (2009) The use of $\delta^{15}\text{N}$ in assessing sewage stress on coral reefs. *Marine Pollution Bulletin* 58(6), 793–802. doi:10.1016/j.marpolbul.2009.02.008
- Seemann J (2013) The use of ^{13}C and ^{15}N isotope labeling techniques to assess heterotrophy of corals. *Journal of Experimental Marine Biology and Ecology* 442, 88–95. doi:10.1016/j.jembe.2013.01.004
- Seemann J, Carballo-Bolanos R, Berry KL, González CT, Richter C, Leinfelder RR (2012) Importance of heterotrophic adaptations of corals to maintain energy reserves. In 'Proceedings of the 12th international coral reef symposium, 9–13 July 2012, Cairns, Qld, Australia'. (Eds D Yellowlees, TP Hughes) ICRS2012_19A_4, pp. 9–13. (International Society for Reef Studies) Available at https://www.icrs2012.com/proceedings/manuscripts/ICRS2012_19A_4.pdf
- Sherwood OA, Jamieson RE, Edinger EN, Wareham VE (2008) Stable C and N isotopic composition of cold-water corals from the Newfoundland and Labrador continental slope: examination of trophic, depth and spatial effects. *Deep Sea Research Part I: Oceanographic Research Papers* 55(10), 1392–1402. doi:10.1016/j.dsr.2008.05.013
- Sulu R (2007) 'Status of coral reefs in the Southwest Pacific.' (IPS Publications, University of the South Pacific)
- Swart PK, Saied A, Lamb K (2005) Temporal and spatial variation in the $\delta^{15}\text{N}$ and $\delta^{13}\text{C}$ of coral tissue and zooxanthellae in *Montastraea faveolata* collected from the Florida reef tract. *Limnology and Oceanography* 50(4), 1049–1058. doi:10.4319/lo.2005.50.4.1049
- Tanaka Y, Miyajima T, Koike I, Hayashibara T, Ogawa H (2006) Translocation and conservation of organic nitrogen within the coral-zooxanthella symbiotic system of *Acropora pulchra*, as demonstrated by dual isotope-labeling techniques. *Journal of Experimental Marine Biology and Ecology* 336(1), 110–119. doi:10.1016/j.jembe.2006.04.011
- Tanaka Y, Ogawa H, Miyajima T (2010) Effects of nutrient enrichment on the release of dissolved organic carbon and nitrogen by the scleractinian coral *Montipora digitata*. *Coral Reefs* 29(3), 675–682. doi:10.1007/s00338-010-0639-9

- Tremblay P, Maguer JF, Grover R, Ferrier-Pages C (2015) Trophic dynamics of scleractinian corals: stable isotope evidence. *Journal of Experimental Biology* **218**(8), 1223–1234. doi:10.1242/jeb.115303
- Umezawa Y, Miyajima T, Yamamuro M, Kayanne H, Koike I (2002) Fine-scale mapping of land-derived nitrogen in coral reefs by $\delta^{15}\text{N}$ in macroalgae. *Limnology and Oceanography* **47**(5), 1405–1416. doi:10.4319/lo.2002.47.5.1405
- Wang W-L, Yeh H-W (2003) $\delta^{13}\text{C}$ values of marine macroalgae from Taiwan. *Botanical Bulletin of Academia Sinica* **44**, 107–112.
- Wheeler PA, Björnsäter BR (1992) Seasonal fluctuations in tissue nitrogen, phosphorus, and N:P for five macroalgal species common to the Pacific northwest coast. *Journal of Phycology* **28**(1), 1–6. doi:10.1111/j.0022-3646.1992.00001.x
- Williamson JE, Rees TAV (1994) Nutritional interaction in an alga–barnacle association. *Oecologia* **99**(1–2), 16–20. doi:10.1007/BF00317078
- Wong CWM, Duprey NN, Baker DM (2017) New insights on the nitrogen footprint of a coastal megalopolis from coral-hosted *Symbiodinium* $\delta^{15}\text{N}$. *Environmental Science & Technology* **51**(4), 1981–1987. doi:10.1021/acs.est.6b03407
- Wright JT, de Nys R, Steinberg PD (2000) Geographic variation in halogenated furanones from the red alga *Delisea pulchra* and associated herbivores and epiphytes. *Marine Ecology Progress Series* **207**, 227–241. doi:10.3354/meps207227
- Yamamuro M, Kayanne H, Minagawao M (1995) Carbon and nitrogen stable isotopes of primary producers in coral reef ecosystems. *Limnology and Oceanography* **40**(3), 617–621. doi:10.4319/lo.1995.40.3.0617
- Zheng X, Huang L, Lin R, Du J (2015) Roles of epiphytes associated with macroalgae in benthic food web of a eutrophic coastal lagoon. *Continental Shelf Research* **110**, 201–209. doi:10.1016/j.csr.2015.10.013
- Zimba PV, Hopson MS (1997) Quantification of epiphyte removal efficiency from submersed aquatic plants. *Aquatic Botany* **58**(2), 173–179. doi:10.1016/S0304-3770(97)00002-8
- Zweng RC, Koch MS, Bowes G (2018) The role of irradiance and C-use strategies in tropical macroalgae photosynthetic response to ocean acidification. *Scientific Reports* **8**(1), 1–11. doi:10.1038/s41598-018-27333-0

Data availability. The data that support this study will be shared upon reasonable request to the corresponding author.

Conflicts of interest. The authors declare they have no conflicts of interest.

Declaration of funding. This work was funded by CONACYT and the School of Natural Sciences at Macquarie University.

Acknowledgements. We thank Sarah Collison for assistance with sample collection, Lydiane Mattio with macroalgal species identification, Aashi Parikh for assistance in the laboratory, and the Marine Ecology Group at Macquarie University for collegial support.

Author affiliations

^ASchool of Natural Sciences, Macquarie University, Sydney, NSW 2109, Australia.

^BSchool of Environmental and Life Sciences, University of Newcastle, Ourimbah, NSW 2258, Australia.

^CCentre for Tropical Water and Aquatic Ecosystem Research, James Cook University, Cairns, Qld 4879, Australia.